

## Femtosecond Infrared Emission Resulting from Coherent Charge Oscillations in Quantum Wells

A. Bonvalet,<sup>1,2</sup> J. Nagle,<sup>3</sup> V. Berger,<sup>3</sup> A. Migus,<sup>1</sup> J.-L. Martin,<sup>1</sup> and M. Joffre<sup>1</sup>

<sup>1</sup>Laboratoire d'Optique Appliquée, Ecole Nationale Supérieure de Technique Avancées, Ecole Polytechnique, Centre National de la Recherche Scientifique URA 1406-INSERM U451, F-91125 Palaiseau Cedex, France

<sup>2</sup>SBE/DBCM Commissariat à l'Energie Atomique-Saclay, F-91191 Gif-sur-Yvette, France

<sup>3</sup>Laboratoire Central de Recherches, Thomson-CSF, F-91404 Orsay Cedex, France

(Received 27 February 1996)

We excite quantum beats in a quantum well using 12 fs optical pulses. The resulting coherent charge oscillation, in the tens-of-tetrahertz range, radiates a corresponding infrared electromagnetic wave which is monitored through heterodyne detection using as a reference a nearly single-cycle infrared pulse. The direct observation of this wave-packet oscillation yields information on the relaxation of intersubband coherence in quantum wells. Furthermore, the experiment yields simultaneously the femtosecond dynamics of both diagonal and off-diagonal matrix elements of the density operator. [S0031-9007(96)00349-3]

PACS numbers: 73.20.Dx, 42.50.Md, 78.47.+p

The detection of the electromagnetic wave radiated by the oscillation of a wave packet in a quantum-well structure [1,2] has been an important step forward in semiconductor physics in that it demonstrated unambiguously the existence of coherent charge oscillations in such systems. However, up to now, the coherent charge oscillation in the conduction band has been observed only between different quantum wells, e.g., in a structure made of two adjacent wells of different widths, placed in an electric field so that tunneling could take place [1]. Another related example has been the observation of Bloch oscillations in a superlattice in the Wannier-Stark regime [2]. In both cases, a coherent superposition of states was prepared through excitation by a 100 fs pulse. The subsequent far-IR emission was detected using standard electro-optic gating techniques [3], limiting the bandpass to a few THz at most, i.e., to transition energies of about 10 meV. In this Letter, we report on the light emission associated with wave-packet oscillations of electrons within a *single well*, associated with much higher oscillating frequencies. Because of the larger transition energy, in the 100 meV range, the wave packet oscillation can now be observed even at room temperature. These energies, above the LO-phonon energy, also correspond to a totally different physical regime. The observation of wave-packet oscillations at such high frequencies was made possible through the use of shorter pulses of duration 12 fs, and also by using light detection in the mid-infrared in a coherent heterodyne detection scheme based on time-domain interferometry with an ultrashort mid-IR reference pulse. Furthermore, we show in this Letter that we measure not only the coherence, but also the population decay, thus fully determining the time evolution of the density operator after an ultrashort impulsive excitation.

The creation of a wave packet involves the simultaneous excitation of more than one energy level, all within the coherent bandwidth of a short laser pulse. In our

case, shown in the inset of Fig. 1, two energy levels of an asymmetric multiple quantum well (MQW) structure are excited through optical transitions from the valence band. The wave function just after pump absorption is then a coherent linear superposition of both excited states  $E_1$  and  $E_2$ . The difference in Bohr frequencies results in a quantum beat oscillating at the transition frequency  $\omega_{21}$  between the two states. One consequence of this beat is a coherent charge oscillation [1], giving rise to an emitted mid-IR electromagnetic wave. This mid-IR emission can also be viewed as difference-frequency mixing in a resonant medium. Therefore, since it originates from a second-order nonlinear process, the emission can occur only in noncentrosymmetric systems, hence our initial choice of a compositionally asymmetric quantum well [4],

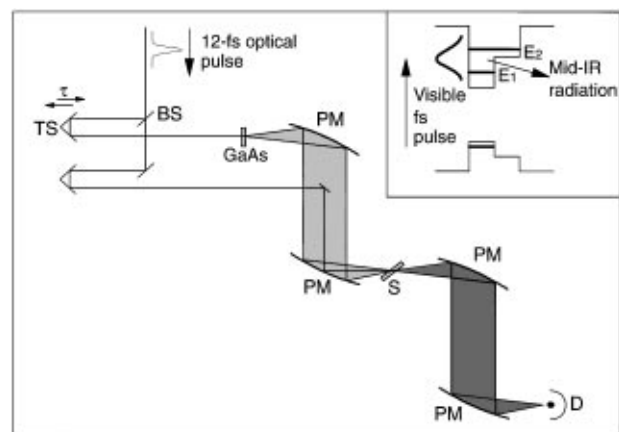


FIG. 1. Experimental setup. BS, beam splitter; TS, translation stage; PM, gold-coated parabolic mirror; S, sample; D, HgCdTe detector. The inset shows the sample excitation condition, here in the case of an asymmetric quantum well. The short pump pulse excites a coherent superposition of  $E_1$  and  $E_2$  from the valence state  $HH_1$ , resulting in a midinfrared emission.

whose structure was optimized [5] to enhance the product of matrix elements involved in the infrared emission. The density matrix of the system in the presence of the exciting pulse is assumed to obey the Bloch equation, which takes into account population and coherence relaxation. Using a three-level model and developing the density matrix up to second order in the electric field  $E(t)$ , we find

$$\rho_{ij}^{(2)}(t) = -\mu_{i0}\mu_{0j}G_{ij}(t) \otimes E(t)\{[G_{0j}(t) + G_{i0}(t)] \otimes E(t)\}, \quad (1)$$

where  $\mu_{nm}$  is the dipolar matrix element and  $G_{nm}(t) = i/\hbar\Theta(t)\exp(-i\omega_{nm}t - \Gamma_{nm}t)$  is the Green function associated with the optical transition from states  $n$  to  $m$ .  $\Theta(t)$  is the Heaviside function.  $\Gamma_{nm}$  is the decay rate corresponding, respectively, to dephasing when  $n \neq m$  and to population relaxation when  $n = m$ . Equation (1) can be numerically computed in a straightforward manner using a few Fourier transforms and simple multiplications in frequency and time domains, successively [6]. In case the pump pulse is much shorter than all relaxation times and if its spectrum encompasses both states  $E_1$  and  $E_2$ , the induced coherence  $\rho_{21}^{(2)}(t)$  is directly proportional to the Green function  $G_{21}(t) \propto \Theta(t)\exp(-i\omega_{21}t - t/T_2)$ , where  $T_2 = 1/\Gamma_{21}$  is the dephasing time. As a result of this evolution of the density operator, a time-dependent polarization is induced in the system  $P^{(2)}(t) = \mu_{12}\rho_{21}(t)$ , whose oscillation in time is responsible for the mid-IR radiation. Therefore, the mid-IR emission oscillates at frequency  $\omega_{21}$  and decays with a time constant  $T_2$ . For the sake of simplicity, Eq. (1) includes only optical transitions from the heavy hole  $\text{HH}_1$  state, while  $\rho_{21}$  really involves a summation over optical transitions from all hole states. When the pump pulse is infinitely short, this summation is proportional to  $\sum_j \langle E_2 | \text{HH}_j \rangle \langle \text{HH}_j | E_1 \rangle = 0$ , since the hole-state envelope functions form a complete set of the Hilbert space corresponding to motion along the growth axis, and  $\langle E_2 | E_1 \rangle = 0$ . Fortunately, we find that this sum rule does not fully apply when the finite pulse spectral width is taken into account. A nonzero contribution can be obtained corresponding to up to a few percent of the  $\text{HH}_1$  contribution alone. Note that a sum over all  $\mathbf{k}$  states must also be performed. These effects, although quantitatively important, will be discussed elsewhere and we now concentrate on the mid-IR emission itself.

Figure 1 shows the experimental setup. The incident laser beam, delivered by a 12 fs Ti:sapphire oscillator [7], is split in two parts. One of the two beams is focused onto the MQW sample using a small fraction of the aperture of a gold-coated off-axis parabolic mirror. The mid-IR radiation emitted by the sample is collected using another parabolic mirror and is then focused on a time-integrating HgCdTe detector, connected to a lock-in amplifier. This part of the setup allows us only to measure the total energy of the emitted radiation. However, a complete determination of the profile of the emitted electric field can be performed using heterodyne methods. To achieve

this purpose, the second 800 nm beam goes through a delay stage and is focused using a 5 cm spherical mirror onto a  $[1\bar{1}0]$  GaAs sample in order to generate through optical rectification a quasi-single-cycle mid-IR reference pulse [8]. Because of its larger wavelength, the diffraction-limited divergence of the reference beam is about ten to fifteen times larger than that of the 800 nm beam [9], leading to a much larger beam diameter after collection by a parabolic mirror. It is therefore possible to focus with negligible loss this reference beam onto the MQW sample using the same parabolic mirror that was used for the pump. Assuming the reference pulse is unaffected by transmission through the sample [10], the system is equivalent to an infrared dispersive Fourier-transform spectrometer [11] since the reference pulse and the emission generated by the MQW are collinearly incident on the detector. The measurement of the time integrated signal as a function of time delay yields the linear correlation function between the reference pulse and the emitted radiation.

Figure 2 shows the experimental interference figure obtained with an *undoped* asymmetric quantum well. Since the reference pulse is much shorter than the emission duration, the measured correlation corresponds almost directly to the emitted electric field, which in turn is closely related to the induced polarization. It exhibits oscillations, demonstrating the wave packet oscillations inside the quantum well. The oscillation period, 33 fs, corresponds to an intersubband transition energy  $\hbar\omega_{21} = 126$  meV, i.e., an emission wavelength of  $9.8 \mu\text{m}$ . Because of coherence

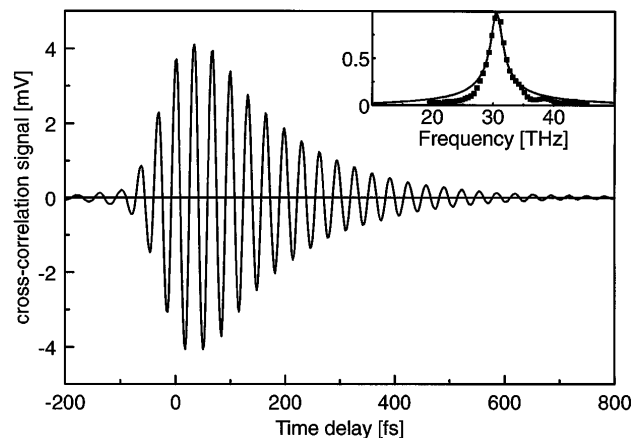


FIG. 2. Midinfrared emission from a MQW structure held at room temperature made of 100 undoped compositionally asymmetric wells  $[\text{Ga}_{0.9}\text{In}_{0.1}\text{As} (4.6 \text{ nm})/\text{GaAs} (5.4 \text{ nm})]$  in AlAs barriers. The data show the correlation between the electric field radiated by the quantum well and the reference electric field emitted by a  $[1\bar{1}0]$  grown GaAs sample. The inset shows the magnitude of the Fourier transform of the experimental data (squares), corrected for the GaAs emission spectrum. The solid line is a calculation based on Eq. (1), using a three-level system excited by a 12 fs pulse, with a fitted dephasing time of 180 fs.

relaxation, the polarization decays as a function of time, with a dephasing time  $T_2 = 180$  fs. As shown in the inset, the Fourier transform of the experimental data is in good agreement with a calculation based on Eq. (1), using the above fitted parameters.

We performed similar experiments on a *doped* quantum well, yielding a dephasing time of about 110 fs, significantly shorter than for undoped wells due to the perturbation brought by the doping process [12]. The transition energy and linewidth thus obtained were in good agreement with cw infrared transmission measurements performed independently on the same sample. Indeed, when the lower state of the quantum well is populated, the very same coherence term  $\rho_{21}$  can also be excited directly at first order, i.e., in a linear experiment using an infrared light source such as a blackbody, of electric field  $E_{\text{IR}}(t)$ :

$$\rho_{21}^{(1)}(t) = \mu_{21} G_{21}(t) \otimes E_{\text{IR}}(t). \quad (2)$$

Therefore, the observation of the wave-packet decay does not yield in principle much information as compared to a linear experiment in this case, although the wave-packet technique allows us to probe a larger  $k$ -space region of the conduction band. However, it is a unique method to study the dynamics of the coherence term between *excited states*, i.e., when the lower state is empty. The alternative existing method, optical pumping of the lower state, is nearly impossible to use when lifetimes are extremely short. This is, for example, the case with infrared intersubband lasers [13], for which the lower-state lifetime is engineered to be as short as possible.

We should also mention our study of *symmetric* quantum wells. Although their infrared emission was greatly reduced by about 1 to 2 orders of magnitude, it was observed not to be exactly zero. Such a small emission, also reported in the case of far-IR radiation [14], demonstrates a noncentrosymmetry, possibly due to band bending associated with a surface electric field, to a slight potential asymmetry, or to valence-band mixing.

We now turn to another attractive feature of our experiment, which is the measurement of both diagonal and off-diagonal matrix elements of the density operator. In the visible spectral domain, such measurements have been performed using other nonlinear optical techniques, such as three-pulse photon echo [15]. However, our technique, which will be shown to provide directly a *simultaneous* measurement of both population and coherence terms, is particularly well suited to the infrared spectral domain. This is achieved using the very same experimental setup shown in Fig. 1, realizing that it also corresponds to a pump-probe configuration, if we only think of the reference beam as a probe beam. Indeed, the detected polarization is the sum of two terms: the second-order nonlinear polarization  $P^{(2)}(t)$ , corresponding to the coherent mid-IR emission already discussed, and the third-order nonlinear polarization  $P^{(3)}(t)$ , which is responsible for changes in the IR probe transmission.

Keeping only the population-term contribution to the third-order polarization [6], the total polarization reads

$$\begin{aligned} P(t) &= P^{(2)}(t) + P^{(3)}(t) \\ &= \mu_{12} \rho_{21}^{(2)}(t) \\ &\quad + G_{21}(t) \otimes \{E_0(t - \tau) [\rho_{11}^{(2)}(t) - \rho_{22}^{(2)}(t)]\}, \quad (3) \end{aligned}$$

where  $\tau$  is the pump-probe time delay,  $E_0(t)$  is the probe pulse electric field, and  $\rho^{(2)}$  is given by Eq. (1). Both terms in the above equation oscillate at frequency  $\omega_{21}$ , yielding a mid-IR emission. The time-integrated second-order detected signal  $\int \text{Re} E_0^*(t - \tau) \dot{P}^{(2)}(t) dt$  exhibits oscillations with respect to the time delay, as already reported in Fig. 2. In contrast, the third-order term is synchronized with the probe pulse, so that the detected signal, now in  $E_0^* E_0$ , does not oscillate with the time delay. This corresponds to the usual pump-probe signal, yielding an increased probe transmission in the case of stimulated emission ( $\rho_{22} > \rho_{11}$ ) and a decreased transmission in the case of induced absorption ( $\rho_{22} < \rho_{11}$ ). The variation of the pump-probe signal with time delay will reflect the population dynamics  $\rho_{22}^{(2)}(\tau) - \rho_{11}^{(2)}(\tau)$  in the limit of an ultrashort probe pulse. An important difference between the two terms of Eq. (3) is that  $P^{(3)}$  is proportional to the probe pulse electric field while  $P^{(2)}$  is independent of it. Therefore, by increasing the *probe pulse energy*, it is possible to go from a second-order effect, as in Fig. 2, to a third-order, or pump-probe effect. Figure 3 corresponds to the intermediate regime, where second-order and third-order terms have comparable magnitudes. This was achieved by using a higher-energy probe pulse, as generated by phase-matched AgGaS<sub>2</sub> instead of GaAs, at the expense of the probe-pulse duration [16]. Furthermore, the sample is now a symmetric quantum well so that the second-order emission is much reduced as compared to an asymmetric quantum well. As expected, the data show not only oscillations corresponding to the second-order term, but also a decrease in probe transmission varying more slowly with time delay. The inset shows the Fourier transform of the experimental data, demonstrating that the contribution from  $P^{(2)}$ , around  $\omega_{21} \approx 30$  THz, and from  $P^{(3)}$ , around zero frequency, are well separated in frequency domain. It is therefore straightforward to isolate each of these two terms through Fourier filtering, keeping only the relevant frequencies. The dotted line in Fig. 3 shows the pump-probe term thus computed, exhibiting a slow decrease in transmission, of magnitude  $\Delta T/T \approx 10^{-3}$ , proportional to the population difference between the upper and lower states  $\rho_{22}^{(2)}(\tau) - \rho_{11}^{(2)}(\tau)$ . The observed rise time is entirely due to the experimental time resolution, limited to about 100 fs since AgGaS<sub>2</sub> produces infrared pulses longer than GaAs [16]. The subsequent population evolution does not show any significant change because the lower level  $E_1$  is excited

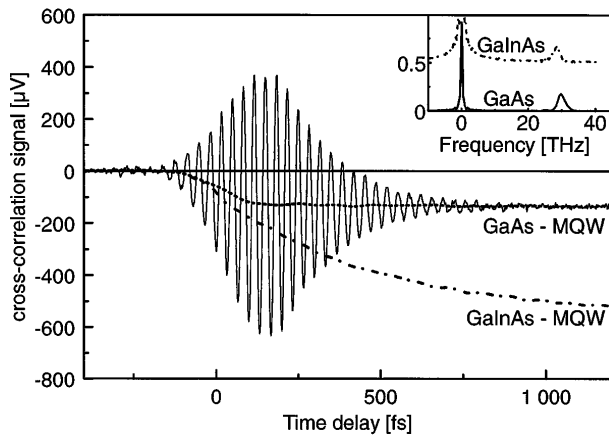


FIG. 3. Signal detected in a structure made of 150 9.2-nm-wide symmetric GaAs quantum wells in AlAs barriers, using AgGaS<sub>2</sub> as the infrared generator for the reference pulse (solid line). The frequency-domain data are shown in the inset (solid line). The population dynamics (dotted line) is extracted by Fourier transforming into the time domain the low-frequency component alone. The same procedure was used to yield the population dynamics in another sample, made of 100 symmetric Ga<sub>0.9</sub>In<sub>0.1</sub>As quantum wells of thickness 10.1 nm in AlAs barriers (dash-dotted line). The dash-dotted line in the inset shows the frequency data for this sample.

much more efficiently by the laser than the higher level. As a consequence, the population dynamics is dominated by  $\rho_{11}$ , whose decay time of about 1 ns makes it roughly constant in the considered time scale. In contrast, the dash-dotted line shows the population dynamics measured using the same technique in a Ga<sub>0.9</sub>In<sub>0.1</sub>As quantum well structure. Because of the lower band gap, the amount of injected electrons is about the same in both states, so that initially  $\rho_{22} \approx \rho_{11}$ , with no change in transmission. The electrons in the upper state then decay exponentially towards the lower state, with a measured time constant  $T_1 = 440$  fs. The coherent emission recorded in the same experiment (not shown) yields a dephasing time  $T_2$  of about 170 fs for this sample. More detailed studies on intersubband relaxation using this technique will be discussed elsewhere.

To summarize, we have observed the coherent mid-IR emission due to quantum beats between the first two electronic states in a quantum well, subsequent to excitation by a 12 fs 800 nm optical pulse. The wave packet oscillation is monitored by measuring the radiated electric field using time-domain linear interferometry with a reference mid-IR ultrashort pulse. The experiment thus provides a direct measurement of the polarization decay of the system, opening up the way to more elaborate related techniques such as coherent control on a 10

fs time scale. Furthermore, we have shown that it is possible to measure in a single experiment both diagonal and off-diagonal matrix elements of the density operator. This should lead to the measurement of key parameters governing the behavior of mid-IR quantum-well devices such as dephasing times and population relaxation times. Although our experiments dealt with electron dynamics in quantum wells, many different studies can also be carried out using similar methods, for example, on vibrational dynamics in molecules.

We are grateful to A. Alexandrou, D. Hulin, and D. Lecompte for fruitful discussions.

- [1] H.G. Roskos, M.C. Nuss, J. Shah, K. Leo, D.A.B. Miller, A. M. Fox, S. Schmitt-Rink, and K. Köhler, *Phys. Rev. Lett.* **68**, 2216 (1992).
- [2] C. Waschke, H.G. Roskos, R. Schwedler, K. Leo, H. Kurz, and K. Köhler, *Phys. Rev. Lett.* **70**, 3319 (1993).
- [3] P.R. Smith, D.H. Auston, and M.C. Nuss, *IEEE J. Quantum Electron.* **24**, 225 (1988).
- [4] M.K. Gurnick and T.A. DeTemple, *IEEE J. Quantum Electron.* **19**, 791 (1983).
- [5] E. Rosencher, A. Fiore, B. Vinter, V. Berger, Ph. Bois, and J. Nagle, *Science* **271**, 168 (1996).
- [6] C. H. Brito-Cruz, J.P. Gordon, P.C. Becker, R.L. Fork, and C.V. Shank, *IEEE J. Quantum Electron.* **24**, 261 (1988).
- [7] Ch. Spielmann, P. F. Curley, T. Brabec, and F. Krausz, *IEEE J. Quantum Electron.* **30**, 1100 (1994).
- [8] A. Bonvalet, M. Joffre, J.-L. Martin, and A. Migus, *Appl. Phys. Lett.* **67**, 2907 (1995).
- [9] M. Joffre, A. Bonvalet, A. Migus, and J.-L. Martin (to be published).
- [10] Third-order optical nonlinearities can cause a small change in absorption of the reference pulse, as will be discussed in the last part of the paper.
- [11] P.R. Griffiths and J.A. de Haseth, *Fourier Transform Infrared Spectrometry*, Chemical Analysis Vol. 83 (John Wiley and Sons, New York, 1986).
- [12] E. B. Dupont, D. Delacourt, D. Papillon, J.-P. Schnell, and M. Papuchon, *Appl. Phys. Lett.* **60**, 2121 (1992).
- [13] J. Faist, F. Capasso, D. L. Sivco, C. Sirtori, A. L. Hutchinson, and A. Y. Cho, *Science* **264**, 553 (1994).
- [14] P. C. M. Planken, M. C. Nuss, I. Brener, K. W. Gossen, M. S. C. Luo, L. Chuang, and L. N. Pfeiffer, *Phys. Rev. Lett.* **69**, 3800 (1992).
- [15] A. M. Weiner, S. De Silvestri, and E. P. Ippen, *J. Opt. Soc. Am. B* **2**, 654 (1985).
- [16] A. Bonvalet, M. Joffre, A. Migus, and J.-L. Martin, in *Proceedings of the CLEO '95 Conference on Lasers and Electro-Optics, Baltimore, Maryland, 1995* (Optical Society of America, Washington, DC, 1995).